HHS Public Access

Author manuscript

Biomaterials. Author manuscript; available in PMC 2018 February 01.

Published in final edited form as:

Biomaterials. 2017 February ; 116: 57–68. doi:10.1016/j.biomaterials.2016.11.033.

Intein-mediated site-specific synthesis of tumor-targeting protein delivery system: Turning PEG dilemma into prodrug-like feature

Yingzhi Chen[a,b], **Meng Zhang**[a,b], **Hongyue Jin**[a], **Yisi Tang**[c], **Huiyuan Wang**[a], **Qin Xu**[c], **Yaping Li**[a], **Feng Li**[d], and **Yongzhuo Huang**[a,*]

[a]Shanghai Institute of Materia Medica, Chinese Academy of Sciences, 501 Hai-ke Rd, Shanghai 201203, China

[b]University of Chinese Academy of Sciences, 19A Yuquan Rd, Beijing 100049, China

[c]Guangzhou University of Chinese Medicine Tropical Medical Institute, 12 Ji-chang Rd, Guangzhou 510405, China

[d]Hampton University School of Pharmacy, Kittrell Hall RM216, Hampton, VA 23668, USA

Abstract

Poor tumor-targeted and cytoplasmic delivery is a bottleneck for protein toxin-based cancer therapy. Ideally, a protein toxin drug should remain stealthy in circulation for prolonged half-life and reduced side toxicity, but turn activated at tumor. PEGylation is a solution to achieve the first goal, but creates a hurdle for the second because PEG rejects interaction between the drugs and tumor cells therein. Such PEG dilemma is an unsolved problem in protein delivery. Herein proposed is a concept of turning PEG dilemma into prodrug-like feature. A site-selectively PEGylated, gelatinase-triggered cell-penetrating trichosanthin protein delivery system is developed with three specific aims. The first is to develop an intein-based ligation method for achieving site-specific modification of protein toxins. The second is to develop a prodrug feature that renders protein toxins remaining stealthy in blood for reduced side toxicity and improved EPR effect. The third is to develop a gelatinase activatable cell-penetration strategy for enhanced tumor targeting and cytoplasmic delivery. Of note, site-specific modification is a big challenge in protein drug research, especially for such a complicated, multifunctional protein delivery system. We successfully develop a protocol for constructing a macromolecular prodrug system with intein-mediated ligation synthesis. With an on-column process of purification and intein-mediated cleavage, the site-specific PEGylation then can be readily achieved by conjugation with the activated C-terminus, thus constructing a PEG-capped, cell-penetrating trichosanthin system with a gelatinase-cleavable linker that enables tumor-specific activation of cytoplasmic delivery. It provides a promising method to address the PEG dilemma for enhanced protein drug delivery, and importantly, a facile protocol for site-specific modification of such a class of protein drugs for improving their druggability and industrial translation.

*Corresponding author: yzhuang@simm.ac.cn (Y. Huang).

Keywords

Intein-mediated protein ligation (IPL); Protein toxin; Trichosanthin; Site-specific PEGylation; Gelatinase; Cell-penetrating peptide

1. Introduction

Tumor-specific cytoplasmic delivery of protein toxins remains two formidable hurdles to reach the action site (e.g., cytoplasm or subcellular organelles). First, the protein drugs must overcome the rapid degradation and clearance from blood circulation. Second, they must be able to penetrate into the targeted cells and enter the cytoplasm. PEGylation is a typical strategy applied in protein delivery for improving the serum stability and pharmacokinetic profiles as well as reducing immunogenicity [1]. However, the conjugated PEG chains also prevent the interaction between the protein drugs and the targeted cells, leading to poor cellular uptake; this so-called PEG dilemma often yields unproductive treatment outcomes [2].

As a case in point, PEGylation methods are hardly used in ribosome-inactivating proteins (RIPs, aka protein toxins) delivery due to this dilemma, which significantly compromised the antitumor activity [3,4]. Protein toxins, represented by trichosanthin (TCS), possess the N-glycosidase activity, with ability to inactivate the ribosome and inhibit protein synthesis, thereby causing cell death [5]. Unlike most small chemotherapeutics typically with IC_{50} values at a nanomolar level (roughly $10^{4–5}$ molecules/cell), one single molecule of protein toxin can kill a tumor cell as long as it can enter the cytoplasm [6]. However, the majority of currently investigated plant protein toxins in oncology belong to Type I RIPs, which are poorly druggable, characterized by short half-life, low tumor accumulation, strong immunogenicity, and much worse, poor cell permeability [7]. PEGylation can solve the major problems, but it nevertheless aggravates the cell-impermeability [4]. In this case, PEG dilemma virtually leaves the protein toxin drugs unworkable. However, such PEGylation shielding strategy was proposed for use for prodrug-like design [8]. Enlightened by this protease-activable, PEG-associated inactivation feature, we developed an activatable cell-penetrating protein toxin delivery system for improving the druggability and therapy efficacy, by which the toxins could be prevented from normal cell entry, and prolong half-life for facilitating tumor-targeting via EPR effect and reduce side toxicity.

Next, we applied a tumor-specifically activatable dePEGylation design by using a gelatinase-cleavable linker between the PEG and protein toxin. With the detachment of PEG, the toxin reinstalls its activity for killing the tumor cells. However, the poorly cell-permeable protein toxins are hard to achieve efficient cytoplasmic delivery. We thus introduced a cell-penetrating peptide (CPP) to a toxin for enhanced intracellular transduction. The CPP was conjugated to PEG via a gelatinase-cleavable linker, thereby constructing an activatable cell-penetrating toxin.

Tumor-associated protease-activatable CPP-based strategy has been used in nanoparticulate drug delivery systems [9–11]. However, its application in protein toxins has been rarely reported. Conventionally, protein PEGylation is hard to achieve site-specification, generally

yielding heterogeneous products and consequently leading to protease-triggered action hard to control and predict. A common strategy for site-selective conjugation is to prepare a recombinant plasmid that encodes a terminal-cysteine fusion protein, which nevertheless could readily form dimers during the expression and purification. Intein-mediated protein ligation (IPL) has been developed for untagged protein expression and protein modification [12,13]. In this work, an IPL method was explored for its use in protein toxin drug development, with combination of genetic modification. The toxin-intein fusion protein is subjected to thiol-induced cleavage, yielding an active thioester or thiol at the C-terminus. The thioester or thiol group can be further used for site-specific conjugation with any modifier (e.g., peptide or PEG) bearing sulfide group or maleimide (Scheme 1). An advantage of this technique is that the protein purification, activation and conjugation can be done with one or two-step on-column process.

We developed a gelatinase (e.g., MMP-2) activatable cell-penetrating TCS delivery system, which possessed several features. First, the recombinant cell-penetrating TCS is fused at its C-terminus with the multifunctional sequence, including a CPP, an MMP-2 substrate peptide (MSP), and intein tag. Through intein-mediated synthesis, a PEG molecule is site-specifically conjugated to the rTCS via the MSP linker. Second, PEG chain caps the CPP, rendering a prodrug-like inactivation nature. Third, upon the activation by the tumor-associated MMP-2 that can cleave the MSP linker and release the CPP-TCS, the pharmacological action is reinstalled (Scheme 2). By this mean, it provides a potential solution to the sequential demands of stealth and penetration in protein drug delivery.

2. Results and discussion

2.1. Protein expression and purification

TCS is a 27-kDa Type I RIP, derived from the Chinese herb *Tian Hua Fen*, the root of *Trichosanthes kirilowii Maxim*. TCS has been approved in China for clinical use in gynecology, including ectopic pregnancies, hydatidiform moles, chorionic epithelioma, and abortion. In addition, TCS possesses high antitumor activity that is related to its ribosome-inactivating cytotoxicity, with great promise for cancer therapy [14]. However, like other plant toxins, TCS is poorly cell permeable and with high incident of antigenicity [4,15].

Low molecular weight protamine (LMWP, peptide sequence: VSRRRRRRGGRRRR) is a CPP originally derived from protamine (an FDA-approved drug) [16]. Importantly, the safety and biocompatibility of LMWP have been demonstrated in animal studies including dogs and rats [17,18]. The potent cell penetration ability of LMWP for drug delivery has been confirmed in our previous studies [19,20]. Therefore, it was selected for promoting TCS cytoplasmic delivery.

We constructed two recombinant plasmids pTXB1-TCS and pTXB1-TLM to express rTCS and rTCS-LMWP-MSP (rTLM) fusion protein using the IMPACT (Intein-Mediated Purification with Affinity Chitin-binding Tag) system [13]. The rTCS or rTLM, fused with a C-terminal self-cleavable intein tag, was expressed from *E. coli*. The intein tag includes the intein sequence (22 kDa) and a chitin-binding domain (CBD, 6 kDa). The purification and thiol-induced intein tag cleavage can be simply conducted by using one single on-column

process. Importantly, either thioester or thiol group can be introduced to the C-terminus of the proteins, depending on which kind of a cleavage agent is used (schematic illustration in Fig. S1, Supporting information).

The rTCS-Intein-CBD and rTLM-Intein-CBD were about 55 and 58 kDa, respectively. Both proteins were expressed in *E. coli* with high yields in a soluble form, as indicated by the bands between 50 and 60 kDa in the IPTG-induced bacterial and *E. coli* lysate (Fig. S2A–B, lane 2–3). The fusion proteins were able to bind onto the chitin column to perform the chitin-affinity purification. After cleavage from intein by using 2- mercaptoethanesulfonic acid (MESNA) or cysteine, the purified rTCS or rTLM showed a molecular weight of 27 kDa or 30 kDa approximately (Fig. S2A–B, lane 5); rTCS possessed a C-terminal thioester and rTLM a C-terminal cysteine. The yield of rTCS and rTLM was around 25 mg and 30 mg per liter of bacterial culture.

2.2. Synthesis and separation of rTCS-LMWP and rTLM-PEG conjugate

The rTCS-LMWP conjugate showed the molecular mass of about 29 kDa, slightly larger than rTCS. Because the ligation rate was >90%, determined by a gel analyzer (Fig. S3A), the product, containing very minor unmodified rTCS, was used for subsequent studies without further purification, whereas the extra peptide was removed by using a desalting column (Fig. S3B). The rTCS-LMWP conjugate was used as a control.

The purified, intein-cleaved rTLM fusion protein containing a C-terminal cysteine was used for site-specific PEGylation with maleimide-PEG. The PEGylation efficiency was measured to be approximately 85% by a gel analyzer (Fig. S3C). Because PEG shields the cationic charges of the rTLM, the PEGylated rTLM can be separated using a cation-exchange chromatography. The rTLM-PEG was eluted from the column at a NaCl concentration about 0.3 M, whereas unPEGylated rTLM eluted with higher salt concentration (Fig. S3D). The purified conjugates were characterized by SDS-PAGE electrophoresis (Fig. 1A) and MALDI-TOF-MS (Fig. 1B), confirming the success of intein-mediated protein modification. The purity of rTCS, rTCS-LMWP and rTLM-PEG was further assessed by size exclusion chromatography, showing a purity of over 90% (Fig. 1C). The size of rTCS and rTLM-PEG conjugate was measured as 6 and 8 nm, respectively, using dynamic lightening scattering (DLS) (Fig. S4), indicating rTLM-PEG had larger hydrodynamic size than unmodified rTCS due to the PEG corona.

2.3. MMP-2-triggered cytotoxicity of rTLM-PEG

To investigate the cleavability of PEG from rTLM-PEG at the MSP site so as to achieve MMP-2-triggered activation, rTLM-PEG was incubated with the HT1080 cell-conditioned medium containing secreted MMP-2 (Fig. 2A). A majority of rTLM-PEG was successfully cleaved, and the cleavage rate was >80% measured by gel imaging analysis. By contrast, the rTCS-LMWP-PEG (rTL-PEG) conjugate without MSP sequence showed very minor cleavage (Fig. 2B).

The cytotoxicity studies were carried out using HT1080 tumor cells (MMP-2 overexpression) and non-tumoral HUVEC cells (MMP-2 low expression). Due to its non-selective cell penetration, rTCS-LMWP showed enhanced cytotoxicity in both HT1080 cells

and HUVEC cells compared to rTCS that is poorly cell-permeable. Importantly, the activatable rTLM-PEG showed similar cytotoxicity as rTCS-LMWP in HT1080 cells after MMP-2-triggered dePEGylation. On the contrary, the non-activatable conjugate rTL-PEG (without MSP linker) was less cytotoxicity in both cell lines, indicating PEG effectively shielded CPP and inhibited cell entry (Fig. 2C and D). The IC_{50} values of rTCS, rTCS-LMWP, rTLM-PEG and rTL-PEG were 1530, 138, 127 and 5030 nM in HT1080 cells, respectively, whereas they were 9.5, 0.8, 8.4 and 8.7 μM in the HUVEC cells, respectively. Therefore, in the MMP-2 positive tumor cells, rTLM-PEG displayed high antitumor activity similar to the cell-penetrating rTCS-LMWP, but in the MMP-2 negative HUVEC cells, rTLM-PEG remained inactive. The results confirmed the tumor-selective action of rTLM-PEG, and the success of MMP-2 activatable cell penetration as well. It demonstrated the prodrug-like feature and the feasibility for use for tumor-targeting delivery.

2.4. Kinetic profile of MMP-2-triggered dePEGylation

Kinetic profile of MMP-2-triggered de-PEGylation was measured by incubating rTLM-PEG with HT1080 cells. SDS-PAGE showed rTLM-PEG was efficiently cleaved by exposure to MMP-2. The majority of incubated rTLM-PEG was cleaved to a cell-penetrating form rTLM (approximate 29 kDa) after 48-h incubation (>70%, Fig. 3).

2.5. Cellular uptake

The FITC-labeled rTLM-PEG pre-activated by the MMP-2 containing medium showed much higher cell uptake efficiency in both cell lines than the inactive form observed in fluorescence imaging (Fig. 4A), suggesting that CPP-facilitated penetration ability can be restored by MMP-2-triggered dePEGylation (Fig. 4B). Consistently, the quantitative results determined by flow cytometry were also demonstrated that the MMP-2 activated rTLM-PEG had a significantly enhanced cellular uptake efficiency compared to the intact rTLM-PEG (Fig. 4C). Mean fluorescence intensity in the groups treated with the activated rTLM-PEG was 3.1-fold (HT1080) and 7.5-fold (HUVEC) higher than those treated with the inactive form, demonstrating the MMP-2-modulated “on-and-off” of the prodrug-like rTLM-PEG.

2.6. In vivo imaging

The *in vivo* imaging results showed that rTLM-PEG was effectively delivered to the tumor and achieved high accumulation in 4 h (Fig. 5A), presumably owing to the EPR effect-associated tumor targeting. At the 24-h mark, the major organs were collected for *ex vivo* imaging, and still there was substantial fluorescence observed at tumors (Fig. 5B). Kidney and liver are known to be the major metabolism organs for protein drugs [21]. TCS is believed to bind to low-density lipoprotein receptor related protein-1 [22], which is richly present and has important functions in lung [23]. Our results also displayed considerable drug disposition in these organs. It should be noted that the non-modified TCS had low tumor accumulation (Fig. S5).

Of note, the interstitial fluid pressure (IFP) in tumor is a hurdle against the intratumoral diffusion and penetration of drugs [24]. Macromolecules are often poorly diffusive. LMWP has been previously demonstrated for enhanced intratumoral penetration [20]. In this work, the cryosection slices of the tumor were observed using confocal laser scanning microscope.

It was found that rTLM-PEG was distributed into the deep site of tumor (Fig. 5C). The deep penetration of rTLM-PEG was mediated by the deshielded cell-penetrating LMWP peptide.

2.7. Pharmacokinetic assay

The plasma concentration-time profiles of rTCS, rTLM-PEG, and rTL-PEG were shown in Fig. 6. The rTLM-PEG and its non-cleavable counterpart rTL-PEG had similar pharmacokinetic profile, showing slower clearance rate than unmodified rTCS due to the PEG-related prolonged circulation. The mean residence time (MRT) was 47, 94, and 105 min, and AUC was 1584, 7624, and 6377 mg min/L for rTCS, rTLM-PEG, and rTL-PEG, respectively. The clearance (CL_Z) of rTLM-PEG (1 ml/min/g) and rTL-PEG (1 ml/min/g) was significantly slower compared to rTCS (5 ml/min/g). Our results were consistent with the previous pharmacokinetic study on rTCS and non-cleavable rTCS-PEG_{5k} [25].

2.8. Immunogenicity

TCS has been reported of strong immunogenicity [26], which is a major hurdle limiting its clinical application in cancer therapy. PEGylation technique has long been used to not only prolong the half-life of protein drugs but also diminish their immunogenicity, because the hydrophilic and flexible PEG chain can prevent interactions between the drugs and serum components and immune cells [27]. Our results demonstrated that the anti-TCS IgG level in the animals challenged with rTLM-PEG was much lower than that in the rTCS-treated group. The titers of neutralizing antibodies for rTCS and rTLM-PEG were 20,000 and 5000 respectively (Fig. 7A), indicating the reduced immunogenicity and improved safety of rTLM-PEG for cancer therapy. It should be mentioned that subcutaneous route of administration is preferred for antigenicity evaluation than intravenous route because the former one is associated with increased immunogenicity and sensitivity.

Macrophages play a significant role in the body by capturing and presenting antigens and inducing immune responses. The macrophage uptake using murine macrophage cells of rTLM-PEG was thus further investigated. The macrophage uptake of rTLM-PEG was shown to be significantly lower than that of rTCS analyzed by both fluorescent imaging and flow cytometer (Fig. 7B and C). The uptake efficiency of rTCS was 3.5-fold higher than rTLM-PEG (Fig. 7D), suggesting the reduced macrophage capture suppress the interaction with antigen-presenting cells, leading to lower immune responses.

2.9. Cancer treatment

In vivo treatment was performed using the HT1080 tumor-bearing mice model by tail intravenous injection of saline, rTCS, rTCS-LMWP, and rTLM-PEG, with a protein dose of 2.5 mg/kg/2d. As shown in Fig. 8, rTCS-LMWP slightly inhibited the tumor growth in comparison with rTCS and rTL-PEG groups but with no significant difference detected. Although LMWP effectively enhanced cytoplasmic delivery of its cargo protein into the tumor cells, rTCS-LMWP was lack of *in vivo* selectivity and had short circulation. Notably, the activatable rTLM-PEG was found to possess significant higher efficacy of tumor inhibition than its MMP-2 non-cleavable PEGylated counterpart rTL-PEG, with inhibition rate of 77.8% vs. 46.1%. It could account for the MMP-2-mediated activation, and thus trigger CPP-mediated cell penetration after the EPR effect-related tumor preferential

distribution of rTLM-PEG. The treatment efficacy of this system was comparable to our previous studies using antibody-directed protein toxin (gelonin) delivery [28]. It could be further improved for achieving complete tumor regression by combination with small chemo drugs.

The animals in both rTCS and rTCS-LMWP groups lost body weight significantly. On the contrary, the animals treated with rTLM-PEG displayed very minor change in body weight (Fig. 8D). The histological examination showed lung, spleen, and kidney-associated toxicity in the mice treated with rTCS or rTCS-LMWP. The pathological symptoms included: increased thickness of the alveolar walls and disarrangement of epithelial cells in lung; abnormal proliferation of giant cells in spleen; disarrangement and swelling of convoluted tubules and glomerular in kidney; and disarrangement and swelling of hepatic cells in liver (Fig. 8E). The adverse effect was probably caused by the non-specific action on the normal tissues and severe immunogenicity of rTCS and rTCS-LMWP. However, there was very minor change in the group treated with rTLM-PEG. The results demonstrated PEGylation could significantly reduce the unwanted effects by preventing non-specific cell penetration and reducing antigenicity. Therefore, the activatable CPP-toxins significantly improved the anti-tumor treatment of TCS with decreased *in vivo* toxicity.

3. Discussion

Type I RIPs (e.g., TCS) are known to have poor cell permeability and tumor targeting, non-specific toxicity, and strong immunogenicity, which greatly constrain their application in clinical oncology despite of their anti-tumor activity. Generally, the compounds with such nature are classified to be poorly druggable, and advanced pharmaceutical techniques are often used to improve the druggability. The toxins have been undergone clinical trials in a form of antibody-toxin conjugates, aka immunotoxins. By conjugation with antibody, the tumor targeting can be improved. However, there still are some major challenges for achieving effective therapy. First, the immunotoxin conjugates are too large to efficiently diffuse deep into the tumor mass [29,30]. The immunotoxins are prone to bind onto the tumor blood vessels and thereby develop a so-called “binding-site effect” against intratumoral penetration [31]. Second, the immunotoxins are deficient in endosome escape, and not capable of effectively releasing into the cytoplasm [32]. Third, there is a high risk of antigenicity caused by immunotoxins, of which the immunogenicity incidence accounts 50–100% post a treatment cycle for solid tumors [33]. Last but not least, protein modification is an arduous process, and difficult to achieve site-specific conjugation, which yields the heterogeneous final products that is difficult for quality control.

PEGylation is a potential solution to improve the druggability of protein toxins. However, the conventional non-cleavable PEG linkage serves as a double-edged sword in this case. In terms of how to overcome the PEG dilemma, it is still an unsolved problem for macromolecular delivery. The PEG dilemma stems from the contrary requirement at various stages of *in vivo* delivery, i.e., from being inactive (in normal tissues) to active (in tumor tissues). In the blood stream, PEG functions as a stealth cloak, and ideally, should protect protein drugs from enzymatic degradation, binding with serum components, and capture by immune cells, thus yielding minimized interaction with the physiological environments.

Then, it should be activated once reaching its destination (e.g., tumor) by responding to the pathological microenvironments, performing CPP-mediated cytoplasmic transduction. Therefore, the cloaking ability of PEG and cell penetration capacity of CPP must work in coordination in order to achieve the optimal delivery efficiency. By using a protease-activatable method, it is feasible for achieving tumor-specific dePEGylation and deshielding of CPP, and triggering the transition from inactive to active status. Our strategy provides a feasible solution to overcome PEG dilemma that commonly exists in protein delivery, and turns a frown upside down.

Another big challenge lies in multipronged site-precise protein modification. It is an ominous task for using a conventional chemical technology for synthesis of such a complicated protein delivery system comprised of multiple functional elements—the parent protein, CPP, MSP, and PEG. Intein-mediated protein conjugation is a bio-recombinant/chemical combination method, which can conveniently achieve protein site-specific modification. IPL is characterized by the simple process of purification and modification with high product yield. Importantly, due to N-S shift, the thiol side chain in cysteine at N-terminal intein tag exists as a thioester form, thereby preventing intermolecular S-S crosslinking. By contrast, in the conventional method (i.e., directly incorporating a terminal cysteine in recombinant proteins), recombinant proteins are inclined to form dimmers. By taking advantage of intein cleavage, the cysteine then can be exposed as C-terminus and facilitate site-specific conjugation. It has been reported that hydrazide-mediated cleavage in IPL was explored to conduct PEGylation of recombinant interferon [34]. Yet, there was no application of IPL technology reported in protein toxins. In this work, we successfully developed a protocol for site-specific PEGylation of protein toxins and protease-triggerable dePEGylation, demonstrating the great potential of IPL for specific engineering of protein toxins, and especially the benefits for multifunctional modification.

4. Conclusions

We developed a site-specific modification platform for constructing a prodrug-like delivery system to address the poor druggability of protein toxins due to their short half-life, severe immunogenicity, and inefficient cell penetration. We prepared a PEG-capped, cell-penetrating rTCS fusion protein using IPL technique. Based on this method, the TCS fusion protein (rTLM) containing two additional functional domains (i.e., LMWP and MMP-2 substrate) was constructed. The IPL renders site-specific conjugation of rTLM with PEG via its C-terminal MMP-2 substrate as a cleavable linker. The system was preferentially activated at the tumor with overexpressing MMP-2 by dePEGylation, thus triggering CPP-assisted cell penetration. The rTLM-PEG enhanced anti-tumor activity with reduced immunogenicity and systematic toxicity. Our method provides a feasible strategy for improving the druggability and treatment efficacy of protein toxins. Importantly, it offers a potential solution to solving problems of site-specific PEGylation of protein toxins and the PEG dilemma that have been long existed in protein delivery and therapy.

5. Experimental

5.1. Materials

TCS-encoding gene [35] was kindly provided by Prof. Pang-Chui Shaw, The Chinese University of Hong Kong. *E. coli* strain BL21 (DE3) was preserved by our laboratory. The IMPACT (Intein-mediated purification with affinity chitin-binding tag) system, including the expressing vector pTXB1 and chitin resin, was obtained from New England Biolabs (England). Lysogeny Broth (LB) medium was purchased from Oxoid (England). Maleimide-PEG_{5k} was purchased from Jenkem Technology Co., Ltd (Beijing, China). Protein marker and isopropyl β-D-1-thiogalactopyranoside (IPTG) were acquired from Thermo (USA). Bradford and BCA microplate protein assay kit and TMB substrate solution were obtained from Beyotime Institute of Biotechnology (Haimen, China). 3-(4, 5-Dimethylthiazol-2-yl)-2, 5-diphenyltetrazolium bromide (MTT) was purchased from Sigma-Aldrich Co., Ltd (USA). Fetal bovine serums (FBS), Dulbecco's modified Eagle's Medium (DMEM) cell culture medium and 0.25% trypsin-EDTA were purchased from Gibco (USA). All used antibiotics were acquired from Amresco (USA). MESNA and L-cysteine were obtained from J&K Scientific Ltd (Shanghai, China). NHS-Cy5 and flourescein isothiocyanate (FITC) were obtained from Melonepharma Biotechnology Co., Ltd (Dalian, China). All other reagents were of analytical grade from Sinapharm Chemical Reagent Co., Ltd. (Shanghai, China).

5.2. Protein expression

The sequence of low molecular weight protamine (LMWP, VSRRRRRRGGRRRR) and MMP-2 substrate peptide (MSP, PLGLAG) were added to the terminal of TCS by polymerase chain reaction (PCR) to prepare the recombinant gene for the fusion protein recombinant TCS-LMWP-MSP (rTLM). Both TCS and TLM sequence were subcloned to an intein-mediated protein expressing vector pTXB1 at *Nde*I and *Xho*I site to prepare pTCS and pTLM. The recombinant plasmids were transformed into *E. coli* BL21 (DE3) competing cells. Bacteria cultures were incubated at 37 °C in LB medium containing 100 μg/ml ampicillin sodium. Target protein expression was induced at 20 °C overnight by the addition of IPTG at the final concentration of 0.3 mM when OD_{600} reached 0.6–0.8.

5.3. Protein purification

The rTCS or rTCS-LMWP-MSP (rTLM) was expressed and purified using the IMPACT system (NEB) according to the manufacturer's instructions with a few modifications. Briefly, the induced bacterial culture was harvested by centrifugation at 6000 rpm for 20 min and the bacteria were suspended in the column buffer (20 mM Hepes-Na, 500 mM NaCl, 1 mM EDTA, pH 8.5). The suspensions were sonicated and centrifuged by 12,000 rpm at 4 °C for 30 min. The supernatant containing soluble target proteins was loaded on the pre-equilibrated chitin gravity column at a speed of approximately 1 ml/min. The columns were flushed sequentially with 20 column volumes of buffer to remove unbound proteins, and 3 bed volumes of cleavage buffer to perform the on-column cleavage. Specifically, 50 mM MESNA was used as cleavage agent for producing the rTCS with C-terminal thioester group, whereas L-cysteine for introducing a C-terminal cysteine to rTLM. The columns were incubated with the cleavage buffer at 4 °C for 16 h, followed by elution and collection of the target proteins.

5.4. Site-specific conjugation of rTCS-LMWP and rTLM-PEG

The rTCS with a C-terminal thioester was then conjugated with the thiolated LMWP (SH-CVSRRRRRRGGRRRR) at a mole ratio of 1:10 in the reaction buffer (100 mM Tris-HCl, 500 mM NaCl, 10 mM MESNA, pH 8.0) (Fig. S1A). The protein and peptide were incubated at 4 °C overnight. The reaction product was loaded on a SDS-PAGE electrophoresis and analyzed by a gel analyzer (BioRad, USA) to evaluate the ligation efficiency. A desalting column (GE Healthcare, USA) was then used to remove the excess peptide, and the rTCS-LMWP conjugate was collected.

The rTLM with C-terminal cysteine was mixed with the 8-fold molar excessive PEG_{5k}-maleimide (Fig. S1B), and incubated at 4 °C for overnight. The unmodified rTLM and rTLM-PEG were separated by using cation-exchange chromatography (HiTrap SPFF, GE Healthcare) with a salt gradient elution from 0.14 to 1 M NaCl at a rate of 0.02 M/min and a flow rate of 1 ml/min. The PEGylation efficiency and purity of the rTLM-PEG were analyzed by using SDS-PAGE electrophoresis and a gel analyzer.

The final products were analyzed by using the MALDI-TOF-MS (MALDI TOF/TOF 5800 analyzer, AB Sciex, Framingham, MA, USA), size exclusion chromatography (Superdex 75, GE healthcare) and dynamic lightening scattering (Malvern, UK).

5.5. Cell culture

Human fibrosarcoma cell line HT1080 cells and human umbilical vein endothelial cells (HUVEC) were cultured in 25 cm^2 flasks and maintained in a humidified 5% CO_2 incubator at 37 °C, with use of Dulbecco's Modified Eagle Medium (DMEM, Gibco, USA) containing 100 U/ml penicillin and 100 μg/ml streptomycin and 10% FBS (Gibco, USA).

5.6. rTLM-PEG cleaved by MMP-2

The cleavage of rTLM-PEG by the tumor-associated protease MMP-2 was investigated in the HT1080-conditioned medium. The HT1080 cells were seeded into a 6-mm dish with a density of 5×10^6 cells. After 4 h that cells adhered to the dish, the culture medium was replaced with fresh medium without FBS. After 24-h incubation, the medium was collected and centrifuged at 12,000 rpm for 10 min at 4 °C to remove the cell debris. The rTLM-PEG was incubated with the HT1080-conditioned medium at 37 °C for 48 h. The cleavage efficiency of rTLM-PEG by MMP-2 was detected by using SDS-PAGE electrophoresis.

5.7. Kinetic profile of MMP-2-catalyzed dePEGylation

The HT1080 cells were seeded into a 6-mm dish with a density of 5×10^6 cells and incubated for 24 h before treatment with 0.3 mg/ml rTLM-PEG. At different incubation time mark, 80 μl cell medium was taken out and added with 20 μl SDS-PAGE loading buffer to stop the reaction. After 48 h incubation, all samples were loaded to a 12% SDS-PAGE electrophoresis. The MMP-2-catalyzing kinetic profile was analyzed using a gel analyzer.

5.8. In vitro cytotoxicity

The *in vitro* anti-cancer activity of rTCS, rTCS-LMWP and rTLM-PEG were determined by a standard MTT assay in the HUVEC cells and the MMP-2 overexpressed HT1080 cells.

The cells were seeded to 96-well plates at a density of 3000 cells per well 24 h before treatment. The cells were treated with different concentrations of protein toxins for 48 h. At the end of the treatment, 20 μl of MTT (5 mg/ml) solution was added to each well and incubated for additional 4 h. The medium was carefully removed and 200 μl of DMSO was added to each well to dissolve the formazan crystals. The absorbance was measured using a microplate reader (Thermo, USA) at λ = 570 nm. The relative cell viability was calculated according to the following equation:

$$\text{Cell viability } (\%) = (OD_{test} - OD_{DMSO}) / (OD_{control} - OD_{DMSO}) \times 100\%$$

5.9. Western blot

The conditioned culture medium of the HT1080 and HUVEC cells were prepared as described above. The HT1080 and HUVEC cells were lysed by RIPA lysate buffer. The cell lysate and cell medium were collected and adjusted to the same protein concentration by BCA protein assay, and then analyzed with 10% SDS-PAGE electrophoresis. The electrobloted PVDF membranes (Merck Millipore, USA) were incubated with the anti-MMP-2 rabbit monocloning antibody (Cell Signaling Technology, USA) and HRP-labeled goat anti-rabbit secondary antibody (Santa Cruz, USA). The membrane was incubated with ECL substrate solution (Peirce, USA) and then subjected to a gel-imaging system (Biorad, USA).

5.10. Cellular uptake

FITC-labeled rTLM-PEG was incubated in the HT1080-conditioned medium with secreted MMP-2, and then added to the HT1080 or HUVEC cells at a final concentration of 1 μM. After incubation for 4 h, the cells were washed by sodium heparin solution and PBS successively to remove the membrane-bound protein drugs. Following DAPI staining, the cells were imaged using fluorescence microscope (Zeiss, Germany). At the meantime, cells treated by the same way were digested by trypsin and further analyzed by flow cytometer (BD Pharmingen, USA) using FL1 channel.

5.11. In vivo imaging

All the animal experimental procedures were approved by the IACUC. Female Balb/c nude mice (4 weeks old) housed under specific pathogen-free condition were free to access sterilized food pellets and distilled water with 12-h light/dark cycle. The HT1080 cells (1×10^6) were inoculated subcutaneously into the back of each mouse. The HT1080 tumor-bearing mice were intravenously injected with Cy5-labeled rTLM-PEG. The tumor drug accumulation and tissue distribution of rTLM-PEG were observed at designated time points using an IVIS imaging system (Caliper Life Science, USA). At the experimental endpoint (24 h mark), mice were humanely sacrificed, and the major organs (heart, liver, spleen, lung, kidney and tumor) were collected for fluorescence imaging.

The cryosection of tumor was fixed in 4% paraformaldehyde. The tissue slice was then imaged by confocal laser scanning microscope (Olympus, Japan).

5.12. Pharmacokinetics

Sprague Dawley (SD) rats (250–300 g) were divided into three groups (three rats per group): rTCS, rTL-PEG, and rTLM-PEG. Animals were given 7.5 mg/kg Cy5-labeled rTCS, rTLM-PEG and rTL-PEG through tail vain injection. Blood samples of each animal were collected from retro-orbital sinus at different time marks, and the serum of each sample was separated by centrifuge. The plasma concentrations of the drugs were calculated by measuring the fluorescent intensity of each serum sample using a fluorescence spectrophotometer (F4600, Hitachi, Japan). The PK parameters were analyzed with physiologic pharmacokinetic model (statistical moment theory, DAS pharmacokinetic software, Shanghai University of T.C.M, China).

5.13. Immunogenicity

Balb/c mice (6 weeks old) were divided into two groups (five per group): rTCS and rTLM-PEG. Animals were immunized at a dose of 10 μg protein per animal subcutaneously once every week for three times. Blood samples of each animal were collected from orbit seven days after the last immunization and serum was separated by centrifuge. The titer of anti-TCS IgG in serum samples was detected by ELISA assay. Briefly, recombinant TCS was diluted by 50 mM bicarbonate buffer (pH 9.6) to 10 μg/ml and was coated to the bottom of a 96-well high-binding ELISA plate (Santa Cruz, USA) with 100 μl per well for 18 h at 4 °C. After washing with PBS-T for three times, the plate was blocked by PBS-T containing 1% BSA at 37 °C for 1.5 h. Serum samples were diluted by PBS-T containing 0.01% BSA to 1:1000–1,000,000. The diluted serum sample (100 μl/well) was dispensed and incubated at 37 °C for 1 h. After washing three times, each well was incubated with 100 μl of HRP-labeled goat anti-mouse secondary antibody (Santa Cruz, USA) diluted by 1000 folds for 1 h. After secondary antibody was washed by PBS-T for three times, 200 μl of TMB substrate solution was added to each well and incubated for 15 min at 37 °C. The chromogenic reaction was terminated by adding 50 μl of 20% H_2SO_4 to each well. The absorbance was measured using a microplate reader at $\lambda = 450$ nm.

5.14. Macrophage uptake assay

The RAW 264.7 cells were seeded into a 12-well plate with a density of 1×10^5 cells 24 h before cells were incubated with 2 μM FITC-labeled rTCS and rTLM-PEG. After 4 h incubation, cells were washed three time by PBS and imaged by fluorescent microscope (Zeiss, Germany), followed by trypsin digest and analysis by Flow Cytometer (BD Pharmingen, USA).

5.15. In vivo anti-cancer treatment

Balb/c nude mice (3–4 weeks old, 18–20 g) harboring HT1080 tumor were randomly divided into four groups (six per group), treated with saline, rTCS, rTCS-LMWP, rTL-PEG and rTLM-PEG, respectively. When the tumor size reached about 100 mm^3, animals were given a dose of 2.5 mg/kg/2d by tail vain injection over a period of 18 days. The therapeutic effect was evaluated by monitoring the tumor size every two days. The tumor size was calculated according to the following formula:

$$V = \left(W^2 \times L\right)/2$$

where L is the longest diameter and W is the shortest diameter.

During the therapy, animal body weights were monitored. At the end of the experiment, animals were humanely sacrificed and tumors were collected and weighed. The major organs (heart, liver, spleen, lung and kidney) were collected and fixed with 4% paraformaldehyde for paraffin slicing. H&E staining was then performed for histological examination.

5.16. Statistical analyses

The results were shown as mean ± SD (n > 3). Statistical analyses were conducted using ordinary one-way ANOVA test by GraphPad Prism. *p < 0.05; **p < 0.01; ***p < 0.001.

Acknowledgments

This work was supported by 973 Program, China (2014CB931900, 2013CB932503) and NSFC, China (81172996, 81373357, 81422048, 81521005, 81673382). The original TCS plasmid was kindly provided by Prof. Pang-Chui Shaw, The Chinese University of Hong Kong. We also thank National Center for Protein Science Shanghai, CAS, for the technical support at MALDI-TOF MASS Facility.

References

1. Pasut G, Veronese FM. State of the art in PEGylation: the great versatility achieved after forty years of research. J Control Release. 2012; 161:461–472. [PubMed: 22094104]
2. Hatakeyama H, Akita H, Harashima H. The polyethyleneglycol dilemma: advantage and disadvantage of PEGylation of liposomes for systemic genes and nucleic acids delivery to tumors. Biol Pharm Bull. 2013; 36:892–899. [PubMed: 23727912]
3. Bian X, Shen F, Chen Y, Wang B, Deng M, Meng Y. PEGylation of alpha-momorcharin: synthesis and characterization of novel anti-tumor conjugates with therapeutic potential. Biotechnol Lett. 2010; 32:883–890. [PubMed: 20238144]
4. An Q, Lei Y, Jia N, Zhang X, Bai Y, Yi J, et al. Effect of site-directed PEGylation of trichosanthin on its biological activity, immunogenicity, and pharmacokinetics. Biomol Eng. 2007; 24:643–649. [PubMed: 18023612]
5. Endo Y, Mitsui K, Motizuki M, Tsurugi K. The mechanism of action of ricin and related toxic lectins on eukaryotic ribosomes. The site and the characteristics of the modification in 28 S ribosomal RNA caused by the toxins. J Biol Chem. 1987; 262:5908–5912. [PubMed: 3571242]
6. Atkinson SF, Bettinger T, Seymour LW, Behr JP, Ward CM. Conjugation of folate via gelonin carbohydrate residues retains ribosomal-inactivating properties of the toxin and permits targeting to folate receptor positive cells. J Biol Chem. 2001; 276:27930–27935. [PubMed: 11359781]
7. Gilabert-Oriol R, Weng A, Mallinckrodt B, Melzig MF, Fuchs H, Thakur M. Immunotoxins constructed with ribosome-inactivating proteins and their enhancers: a lethal cocktail with tumor specific efficacy. Curr Pharm Des. 2014; 20:6584–6643. [PubMed: 25341935]
8. Stefan N, Zimmermann M, Simon M, Zangemeister-Wittke U, Pluckthun A. Novel prodrug-like fusion toxin with protease-sensitive bioorthogonal PEGylation for tumor targeting. Bioconjug Chem. 2014; 25:2144–2156. [PubMed: 25350699]
9. Zhu L, Wang T, Perche F, Taigind A, Torchilin VP. Enhanced anticancer activity of nanopreparation containing an MMP2-sensitive PEG-drug conjugate and cell-penetrating moiety. Proc Natl Acad Sci U S A. 2013; 110:17047–17052. [PubMed: 24062440]

10. Huang Y, Jiang Y, Wang H, Wang J, Shin MC, Byun Y, et al. Curb challenges of the “Trojan Horse” approach: smart strategies in achieving effective yet safe cell-penetrating peptide-based drug delivery. Adv Drug Deliv Rev. 2013; 65:1299–1315. [PubMed: 23369828]
11. Veiman KL, Kunnapuu K, Lehto T, Kiisholts K, Parn K, Langel U, et al. PEG shielded MMP sensitive CPPs for efficient and tumor specific gene delivery in vivo. J Control Release. 2015; 209:238–247. [PubMed: 25935707]
12. Muir TW. Semisynthesis of proteins by expressed protein ligation. Annu Rev Biochem. 2003; 72:249–289. [PubMed: 12626339]
13. Mitchell SF, Lorsch JR. Protein derivitization-expressed protein ligation. Methods Enzymol. 2014; 536:95–108. [PubMed: 24423270]
14. Fang EF, Zhang CZ, Zhang L, Wong JH, Chan YS, Pan WL, et al. Trichosanthin inhibits breast cancer cell proliferation in both cell lines and nude mice by promotion of apoptosis. PLoS One. 2012; 7:e41592. [PubMed: 22957017]
15. Sha O, Niu J, Ng TB, Cho EY, Fu X, Jiang W. Anti-tumor action of trichosanthin, a type 1 ribosome-inactivating protein, employed in traditional Chinese medicine: a mini review. Cancer Chemother Pharmacol. 2013; 71:1387–1393. [PubMed: 23377374]
16. Chang LC, Lee HF, Yang Z, Yang VC. Low molecular weight protamine (LMWP) as nontoxic heparin/low molecular weight heparin antidote (I): preparation and characterization. AAPS PharmSci. 2001; 3:E17. [PubMed: 11741268]
17. Lee LM, Chang LC, Wrobleski S, Wakefield TW, Yang VC. Low molecular weight protamine as nontoxic heparin/low molecular weight heparin antidote (III): preliminary in vivo evaluation of efficacy and toxicity using a canine model. AAPS PharmSci. 2001; 3:E19. [PubMed: 11741270]
18. Liang JF, Zhen L, Chang LC, Yang VC. A less toxic heparin antagonist–low molecular weight protamine. Biochem Mosc. 2003; 68:116–120.
19. Yang YX, Jiang YF, Wang Z, Liu JH, Yan L, Ye JX, et al. Skin-permeable quaternary nanoparticles with layer-by-layer structure enabling improved gene delivery. J Mater Chem. 2012; 22:10029–10034.
20. Wang H, Zhao Y, Wang H, Gong J, He H, Shin MC, et al. Low-molecular-weight protamine-modified PLGA nanoparticles for overcoming drug-resistant breast cancer. J Control Release. 2014; 192:47–56. [PubMed: 25003794]
21. Webster R, Didier E, Harris P, Siegel N, Stadler J, Tilbury L, et al. PEGylated proteins: evaluation of their safety in the absence of definitive metabolism studies. Drug Metab Dispos. 2007; 35:9–16. [PubMed: 17020954]
22. Jiao Y, Liu W. Low-density lipoprotein receptor-related protein 1 is an essential receptor for trichosanthin in 2 choriocarcinoma cell lines. Biochem Biophys Res Commun. 2010; 391:1579–1584. [PubMed: 19968964]
23. Wujak L, Markart P, Wygrecka M. The low density lipoprotein receptor-related protein (LRP) 1 and its function in lung diseases. Histol Histopathol. 2016:11746.
24. Grantab RH, Tannock IF. Penetration of anticancer drugs through tumour tissue as a function of cellular packing density and interstitial fluid pressure and its modification by bortezomib. BMC Cancer. 2012; 12:214. [PubMed: 22672469]
25. He XH, Shaw PC, Tam SC. Reducing the immunogenicity and improving the in vivo activity of trichosanthin by site-directed pegylation. Life Sci. 1999; 65:355–368. [PubMed: 10421422]
26. An Q, Wei S, Mu S, Zhang X, Lei Y, Zhang W, et al. Mapping the antigenic determinants and reducing the immunogenicity of trichosanthin by site-directed mutagenesis. J Biomed Sci. 2006; 13:637–643. [PubMed: 16977428]
27. De Groot AS, Scott DW. Immunogenicity of protein therapeutics. Trends Immunol. 2007; 28:482–490. [PubMed: 17964218]
28. Shin MC, Zhang J, Min KA, He H, David AE, Huang Y, et al. PTD-modified attempts for enhanced toxin-based Cancer therapy: an in vivo proof-of-concept study. Pharm Res. 2015; 32:2690–2703. [PubMed: 25701313]
29. Lu Y, Yang J, Sega E. Issues related to targeted delivery of proteins and peptides. AAPS J. 2006; 8:E466–E478. [PubMed: 17025264]

30. Rudnick SI, Adams GP. Affinity and avidity in antibody-based tumor targeting. Cancer Biother Radiopharm. 2009; 24:155–161. [PubMed: 19409036]
31. Sung C, Dedrick RL, Hall WA, Johnson PA, Youle RJ. The spatial distribution of immunotoxins in solid tumors: assessment by quantitative autoradiography. Cancer Res. 1993; 53:2092–2099. [PubMed: 8481911]
32. Woodhams J, Lou PJ, Selbo PK, Mosse A, Oukrif D, MacRobert A, et al. Intracellular re-localisation by photochemical internalisation enhances the cytotoxic effect of gelonin–quantitative studies in normal rat liver. J Control Release. 2010; 142:347–353. [PubMed: 19932724]
33. Kreitman RJ. Immunotoxins for targeted cancer therapy. AAPS J. 2006; 8:E532–E551. [PubMed: 17025272]
34. Thom J, Anderson D, McGregor J, Cotton G. Recombinant protein hydrazides: application to site-specific protein PEGylation. Bioconjugcate Chem. 2011; 22:1017–1020.
35. Zhu RH, Ng TB, Yeung HW, Shaw PC. High level synthesis of biologically active recombinant trichosanthin in Escherichia coli. Int J Pept Protein Res. 1992; 39:77–81. [PubMed: 1634332]

Appendix A. Supplementary data

Supplementary data related to this article can be found at http://dx.doi.org/10.1016/j.biomaterials.2016.11.033.

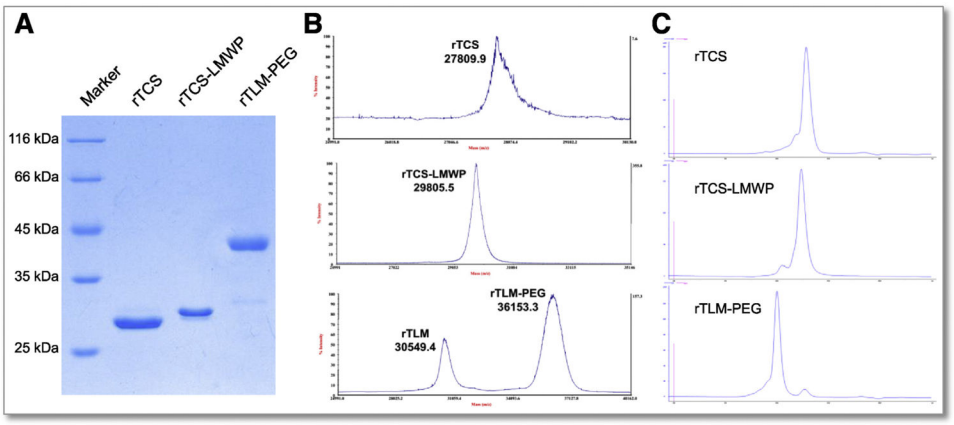

Fig. 1.

Characterization of rTCS, rTCS-LMWP and rTLM-PEG. (A) SDS-PAGE electrophoresis. (B) MALDI-TOF-MS. (C) Purity analysis by size exclusion chromatography.

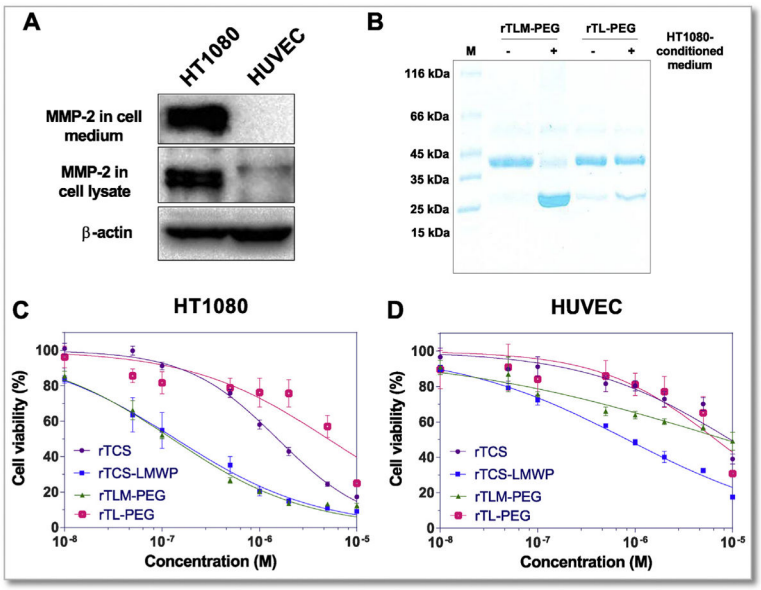

Fig. 2.

MMP-2 activation of rTLM-PEG. (A) MMP-2 expression level in HT1080 and HUVEC cells. (B) MMP-2-mediated cleavage test of rTLM-PEG and rTL-PEG incubated with HT1080-conditioned medium for 48 h. Cytotoxicity of rTCS, rTCS-LMWP conjugate, rTLM-PEG and rTL-PEG in HT1080 cells (C) and HUVEC cells (D).

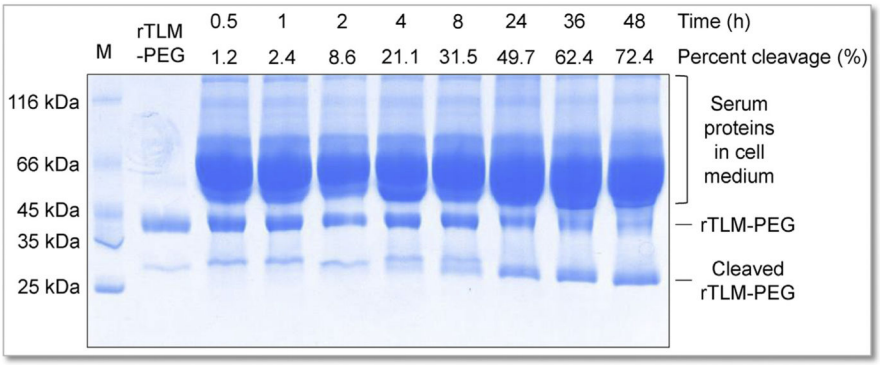

Fig. 3.

Kinetic profile of MMP-2-catalyzed dePEGylation, measured by SDS-PAGE analysis of rTLM-PEG incubated with HT1080 cells at different time.

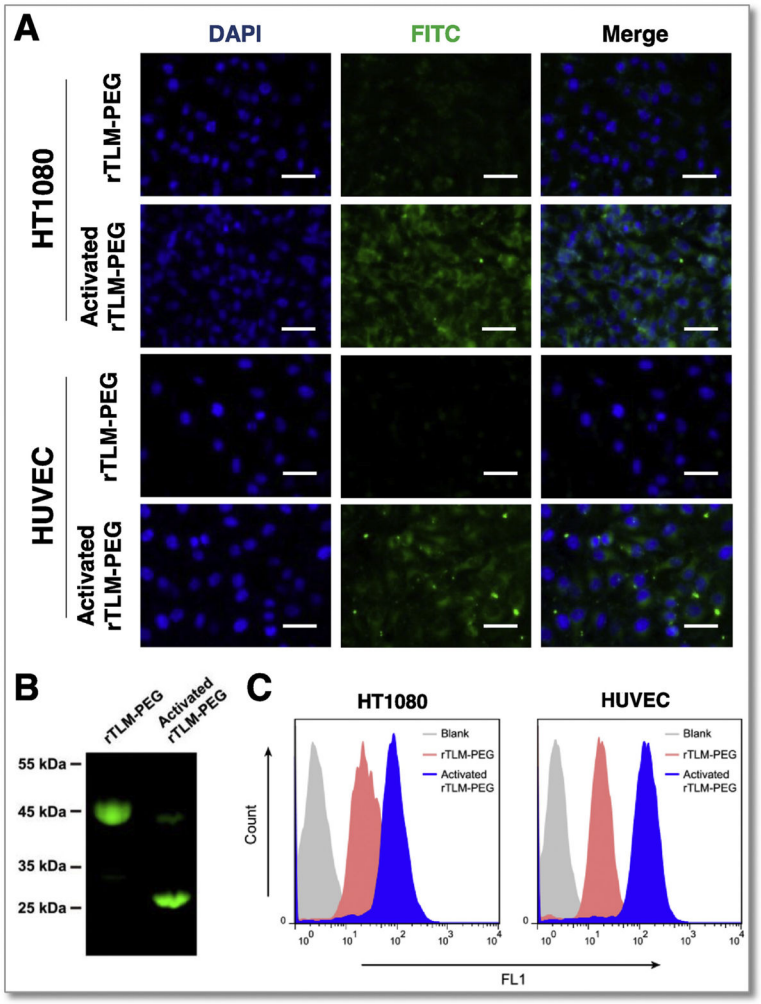

Fig. 4.

Cellular uptake assay. (A) Cellular fluorescence imaging of rTLM-PEG and activated rTLM-PEG in HT1080 and HUVEC cells (scale bar = 50 μm). (B) Cleavage of FITC-labeled rTLM-PEG by MMP-2-containing medium. (C) The cellular uptake efficiency measured by Flow Cytometry.

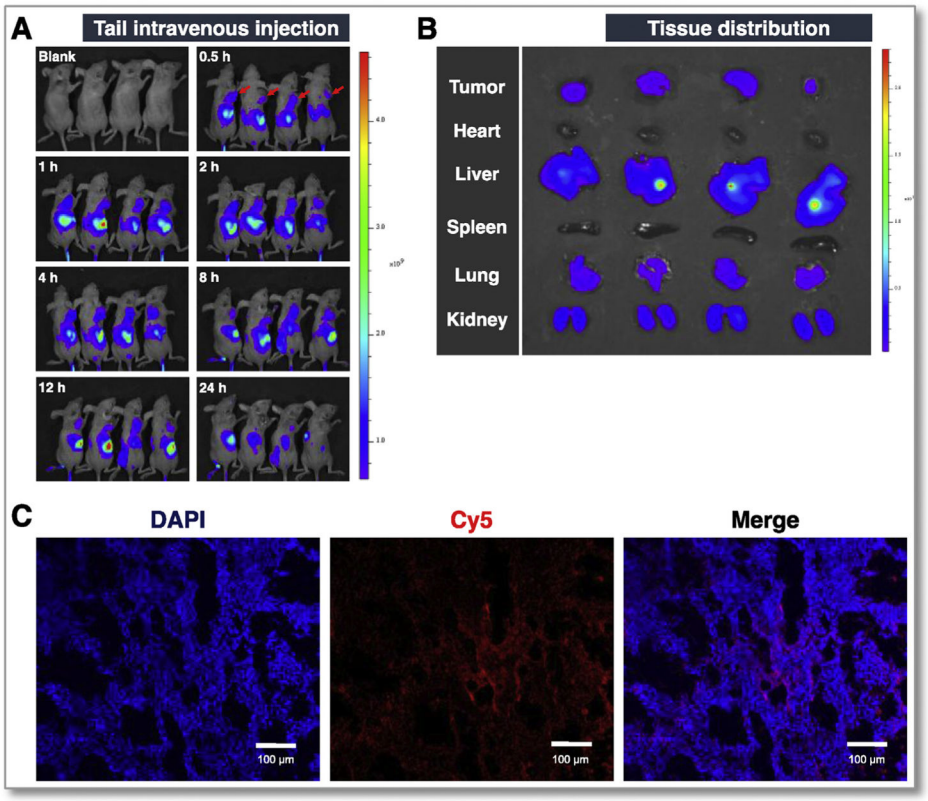

Fig. 5.

In vivo imaging of rTLM-PEG. (A) Drug biodistribution at the designed time points. (B) Tissue distribution at the 24-h mark. (C) Fluorescence image of the slice of tumor (TCS labeled with Cy5, nucleus stained by DAPI).

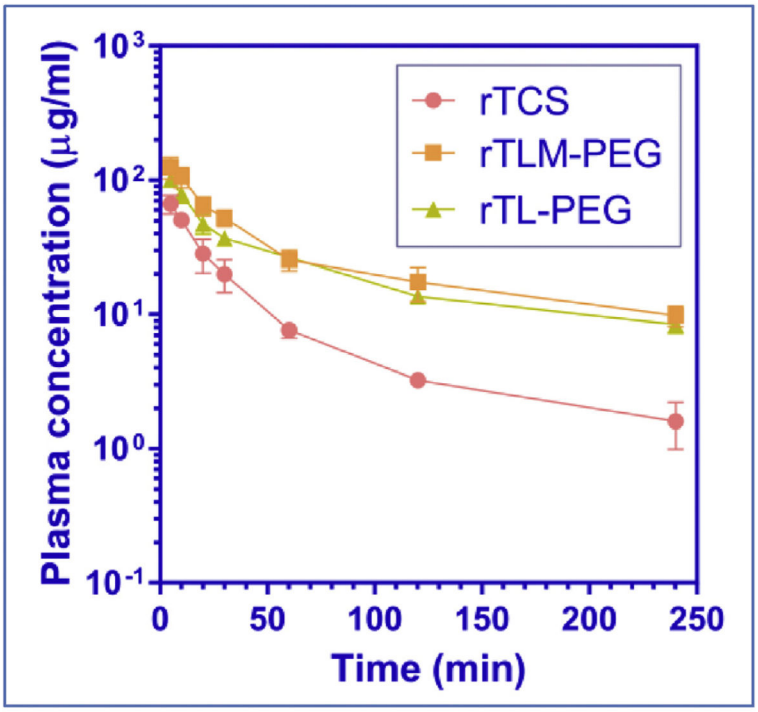

Fig. 6.
Plasma concentration-time profile of rTCS, rTLM-PEG and rTL-PEG measured in rats.

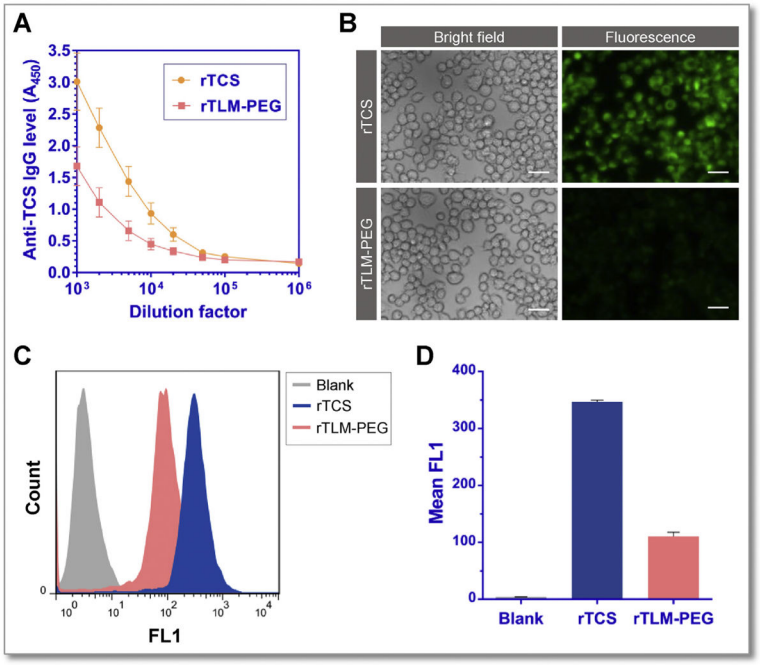

Fig. 7.

Immunogenicity of rTCS and rTLM-PEG. (A) Anti-TCS antibody level measured by ELISA. (B) Fluorescent imaging of RAW 264.7 cells incubated with FITC-labeled rTCS and rTLM-PEG (Scale bar = 20 μm). (C) (D) The cellular uptake efficiency analysis by Flow Cytometer.

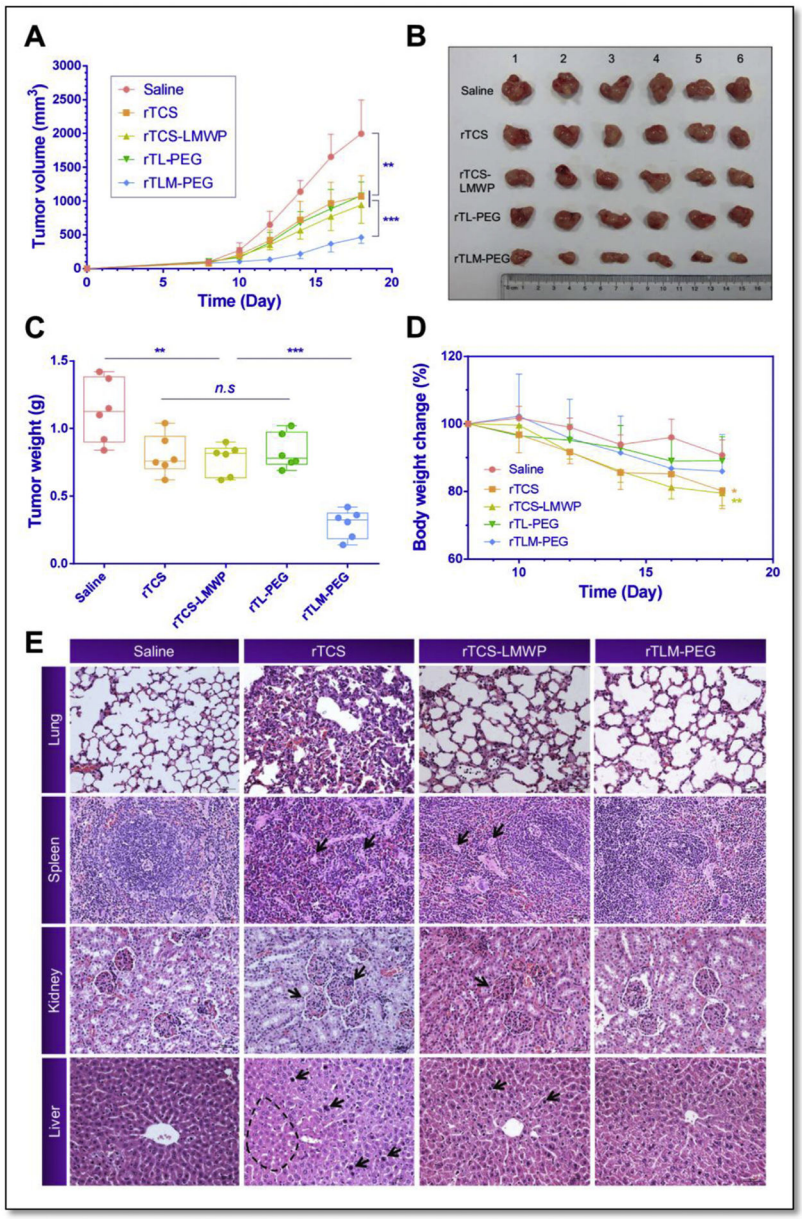

Fig. 8.

In vivo anti-tumor activity study. (A) Tumor sizes in HT1080 tumor bearing nude mice treated with the protein drugs through tail intravenous injection. (B) Tumor sizes and (C) tumor weight measured at the experimental endpoint. (D) Body weight of the treated animals. (E) Histological examination of the major organs. ***P < 0.001, **P < 0.01, *P < 0.05. Points are represented as means ± SD (n = 6).

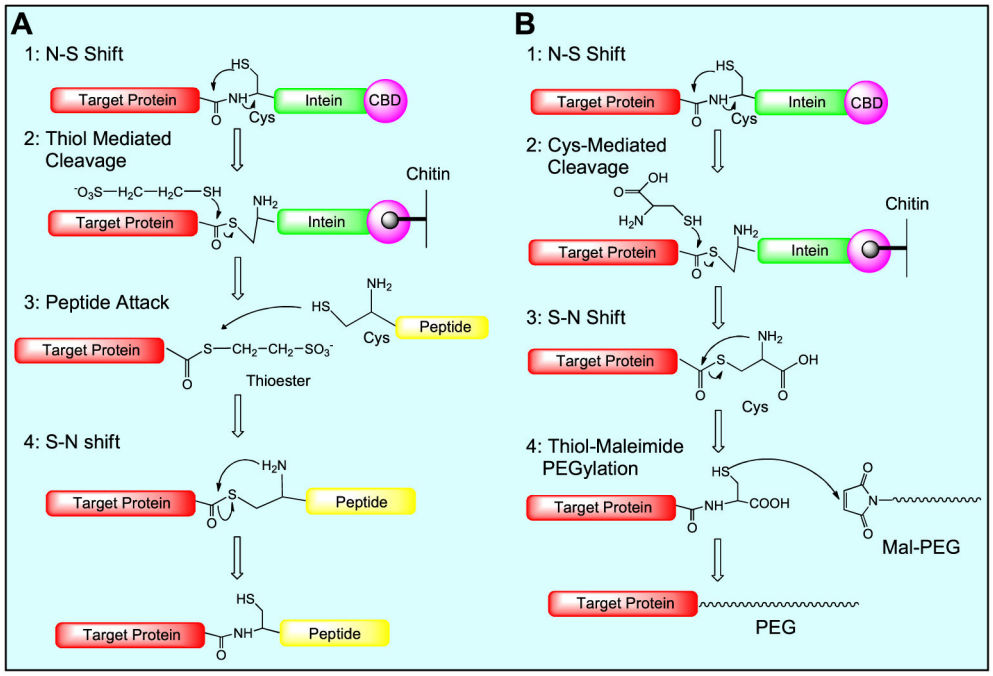

Scheme 1.

Schematic illustration of intein-mediated ligation for site-specific protein modification with either peptide (A) or PEG (B).

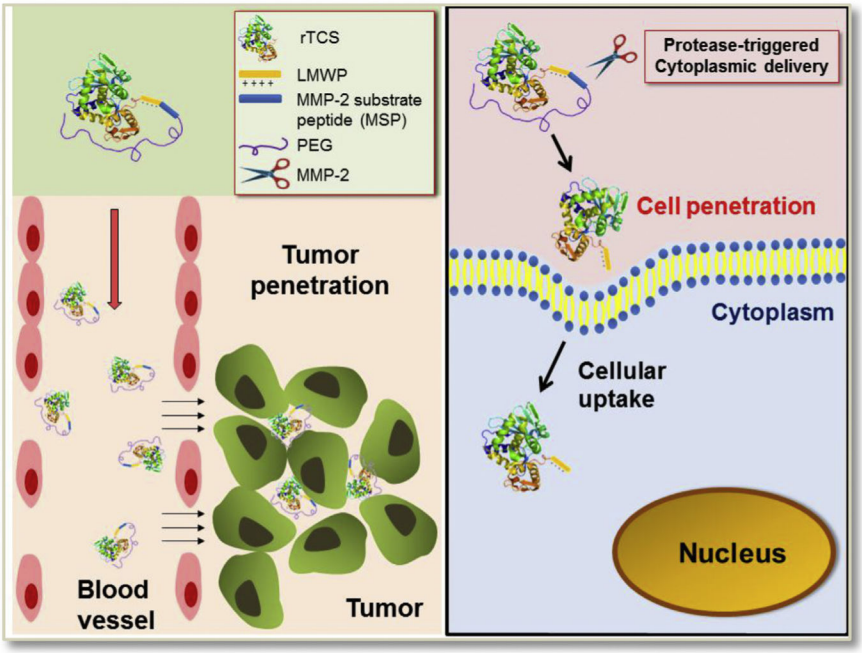

Scheme 2.

Schematic illustration of PEGylated, MMP-2-triggered cell-penetrating TCS tumor-targeted delivery system.